Irrigation Science (2022) 40:359–378
https://doi.org/10.1007/s00271-022-00782-2

ORIGINAL PAPER

A new method for the mathematical modelling of water movement in a surface irrigation system: method and application

Murat Kilic[1]

Received: 2 January 2020 / Accepted: 2 March 2022 / Published online: 21 March 2022

Abstract

Surface irrigation methods need less capital investment and energy than pressurized systems, and therefore they have a wide range of use in many regions. However, inaccurate system design and irrigation applications lead to non-uniform distribution of water in the soil profile. Therefore, the water loss caused by deep percolation increases, and the water application efficiency decreases. In this investigation, a new method was devised for the optimum design of a blocked end furrow system. The new method simulates the movement properties of water in the soil. It analyzes interactively and simultaneously the infiltration characteristics of the soil, the inflow to the furrow and the irrigation water requirement of the crop. The spatio-temporal variation of the wetting pattern which occurs during the water application period and of the components of the wetting pattern can be determined momentarily for any time point during the irrigation application. This process is carried out by running the movement equations of water in the soil, which are described in this investigation. The proposed method was run for two different sample applications of blocked end furrow systems without slope. In the verification process of the model, the sample applications were compared with the results of the USDA SCS method. The results from the two different methods were compared and analyzed in detail. In conclusion, the results from the proposed method gave the optimum solution for different conditions.

Introduction

Poor design and management of surface irrigation systems cause low water application efficiency and the non-uniform water distribution (Esfandiari and Maheshwari 2001; Kilic and Anac 2012). Border, basin and furrow irrigation methods are used nearly with 90% of irrigated crops worldwide (Bristow et al. 2020). The furrow irrigation method does not need high investment cost, and it is relatively easy to design (Walker and Skogerboe 1987; Bristow et al. 2020). Also, this method provides suitable aeration conditions in the soil (Wu et al. 2017).

In Turkey, nearly 75% of water resource potential is used for irrigation. Domestic and industrial use of water follows this with about 15% and 10%, respectively. However, the amount of irrigation water is not adequate in the country (Kanber and Ünlü 2008). As the furrow irrigation method has a lower investment cost than pressurized systems, it is very common in Turkey (Montesinos et al. 2001; Kilic 2020; Kilic and Anac 2010). Water is applied to the soil surface by gravitation.

Inflow rate, irrigation timing, furrow length, cut-off time and infiltration properties of soils are the components which affect the benefit gained from an irrigation system. Likewise, a small amount of deep percolation and run-off volume provides efficient use of deficient resources (Montesinos et al. 2001; Levidow et al. 2014; Pozo et al. 2019; Ebrahimian et al. 2020; Kilic and Tuylu 2010). Heterogeneity in soils and hydraulic properties make the movement of water both on the soil surface and in the soil profile a complex process. A model was developed by Katopodes (1994) for investigating the hydrodynamics of the surface irrigation. The velocity profile of the wave front was investigated, and the two-dimensional finite element approach was used. Dependent variables of furrow irrigation were described using empirical functions by Zerihun et al. (1997a, b). The specific equations were investigated using the regression analysis.

The amount of irrigation water to be applied, inflow, cut-off time and furrow length are components for the better management of the irrigation application. Raghuwanshi

✉ Murat Kilic
kilic.murat@ege.edu.tr

[1] Faculty of Agriculture, Department of Agricultural Structures and Irrigation, Ege University, B/Block, 35100 Bornova, Izmir, Turkey

and Wallender (1999) optimized these decision variables using the seasonal furrow irrigation model and the time series model. Kang et al. (2000) investigated the advance of water, yield production, water distribution uniformity and the water application efficiency in an arid region for maize, using the conventional furrow irrigation (CFI), the fixed furrow irrigation (FFI) and the alternate furrow irrigation (AFI) methods. A mathematical solution procedure was not developed for the above irrigation applications. Valiantzas (2000) investigated the advance of water in furrows using an equation which did not need estimation of the surface storage volume. Esfandiari and Maheshwari (2001) investigated the estimation of advance and recession times and run-off of the Ross, Walker, Strelkoff and Elliott models. In addition, the computational time and volume balance error were evaluated. Montesinos et al. (2001) developed a model for seasonal furrow irrigation. In this process, the economic benefit was maximized by taking into consideration soil properties, climatological data, crop properties and furrow features. The OPTIMEC (EConomic OPTIMization) program was used in this solution, and a calendar was obtained for the irrigation season.

Furrow irrigation applications were simulated by Mailhol et al. (2005) in order to compare the alternative management strategies. It was determined that variations in the infiltration properties of soils reduced the water application efficiency. Khatri and Smith (2006) predicted the infiltration properties of soil using the water advance data, and the MIC—model infiltration curve—was used in this process. Koech et al. (2014) optimized the automated furrow irrigation system under real time conditions. The optimum efficiency was obtained by predicting the infiltration properties and by the management of irrigation data. Ebrahimian (2014) described the infiltration features of different furrow irrigation applications using the IPARM, the two-point method and the INFILT models. The infiltration parameters of the modified Kostiakov equation were predicted by these three different methods. The Richards equation is used indirectly to predict the amount of deep percolation. The soil hydraulic parameters and the crop properties are necessary for running the Richards equation. Selle et al. (2011) estimated the deep percolation using the Richards equation for surface irrigation. It was examined in this investigation whether the soil moisture data could be used to estimate the deep percolation by running the Richards equation. It was indicated that a simple Richards equation was inadequate for this process.

Various simulation models have been developed for surface irrigation systems in different investigations. HYDRUS (2D/3D) and its predecessors SWMS-2D, CHAIN-2D (Šimůnek et al. 2008, 2016), SURDEV (SURface irrigation DESign, operation and Evaluation model) (Jurriens et al. 2001), surface irrigation simulation evaluation and design model (SIRMOD) (Walker 2003), WinSRFR (Bautista et al. 2009, 2012), SURCOS (Burguete et al. 2014), SIDES (Adamala et al. 2014) and surface irrigation simulation, calibration and optimization model (SISCO) (Gillies and Smith 2015) have been used in various investigations of surface irrigation systems. The HYDRUS program simulates the water movement, the multiple solutes and the heat transfer processes using the numerical solution procedure of the Richards equation. Solute and water movement in two dimensions are simulated by SWMS_2D model by solving the Richards equation numerically. This procedure is carried out for the convection–dispersion equation for the solute transport and the saturated–unsaturated water flow. The CHAIN-2D model simulates the water flow, the heat and the solute transport in two dimensions. In this process, the Richards equation is solved numerically. SURDEV model designs, operates and evaluates the surface irrigation methods. SIRMOD model simulates the surface irrigation hydraulics. The program is based on the hydrodynamic model. The WinSRFR program performs the hydraulic analysis of surface irrigation methods. The design, evaluation, simulation and operational analysis are carried out by this model. The SURCOS program simulates the fertigation and irrigation applications in furrows. The solution procedures are carried out by running the transport equation and the 1D-Saint–Venant equations. The SIDES model designs and evaluates the surface irrigation methods. The volume balance approach is used in this process. The SISCO program simulates the surface irrigation methods to the open canal flow. The one-dimensional Saint–Venant equations are run in this process. All of these models require different data sets and configurations with different variables, and each of these methods has a different solution approach and specific data requirements (Dialameh et al. 2018).

Wang et al. (2014) investigated the crop yield and soil water dynamics under furrow irrigation. A two-dimensional model was developed using the CHAIN-2D and EPIC models. Water movement in the soil profile and the spatio-temporal variation of the wetting pattern were not taken into consideration. Delgoda et al. (2016) used the water balance approach to maintain the moisture deficit in the root zone. This process was carried out by the model-based control of irrigation. A linear time series model was obtained using the water balance data. Liu et al. (2019) described surface water flow and solute transport by the zero-inertia and average cross-sectional convention–dispersion equations. It was indicated that numerical oscillations could be eliminated by using suitable time steps. Triggered furrow irrigation was simulated and analyzed by Naghedifar et al. (2020) using the 3D Richards equation and the one-dimensional hydrodynamic form of the Saint–Venant equations. The Richards equation was solved by the coordinate transformation technique. Mazarei et al. (2020) used the WinSRFR model to optimize the inflow rate, the cut-off time and the

field geometry. The fertilizer locations in furrow irrigation were determined using a simulation model by Bristow et al. (2020). The effects of various soil surface treatments and deep drainage were evaluated by the HYDRUS model in furrow systems.

A number of scenarios for design parameters need to be examined to achieve the optimum design and management of an irrigation system. The analytical solution method is another approach to describing the nature of the events in the furrow irrigation. In this investigation, a new method is devised based on the analytical solution technique for the blocked end furrow system. The proposed method was run for the solution of different furrow irrigation applications which were published previously by Yıldırım (2013). The results from the model solution were analyzed and verified in detail.

Method

Horizontal movement of water on the soil surface, infiltration in a vertical direction and the wetted area pattern depending on time constitute the main components of the furrow system in this investigation. All of these components are functions of time, and they have interactions with each other.

In this research, movement of water in a blocked end furrow was investigated in spatio-temporal dimensions. There were two main reasons for choosing the blocked end furrow system. The first reason was that the water applied to the blocked end furrow system cannot flow out of the furrow, and, therefore, all the components which constitute the irrigation application can be determined and analyzed as a whole in the same system. Horizontal movement of water on the furrow surface, vertical infiltration of water into the soil profile and spatio-temporal variation of the wetting pattern which occurs at any time t_0 during the water application period can be evaluated and analyzed as a whole in the same system.

The most important reason was that an application efficiency of over 80% can be achieved if the blocked end furrow system is designed accurately (Yıldırım 2013). This provides an important level of water saving especially in arid and semi-arid regions where surface irrigation systems are applied widely.

The wetted area pattern which occurred depending on both the horizontal movement of water on the soil surface and infiltration of water to the soil profile are shown schematically in Fig. 1 (Walker and Skogerboe 1987; USDA SCS 2012).

The wetted area pattern shows a continuous variation depending on the advance period of the water on the soil surface, the infiltration properties of the soil, the inflow to the furrow, the irrigation water requirement of the crop and the length of the irrigation period.

Horizontal movement of water on the soil surface occurs much faster than infiltration in a vertical direction. Therefore, the wetted area pattern in the soil profile is similar to a quarter of an ellipsoid, the foci of which are on the X axis in the IVth zone of the coordinate system.

The next part of this paper will present a mathematical description of the movement of water both on the soil surface and in the soil profile during a hypothetical irrigation event in a level furrow with blocked end.

Relative movement of water in soil

Movement of water before reaching the end of the furrow constitutes the beginning stage of the process. In other words, the elapsed time from the beginning of the irrigation (T_b) is smaller than the water advance period (T_i): ($T_b < T_i$). The water advance period is the length of time until the water reaches the end of the furrow (USDA SCS 2012; Yıldırım 2013).

In this stage, water is supplied to a blocked end furrow with length L with an inflow q which does not cause erosion.

Movement of water before reaching the end of the furrow is in both horizontal and vertical directions, and both of these components are functions of time. Water movement in the furrow in these conditions is shown schematically in Fig. 2.

In this state, as water advances in the horizontal direction, it infiltrates into the soil at the same time. Water moves on the soil surface with a velocity of $\frac{\partial a_h}{\partial t} = v$. As the total length

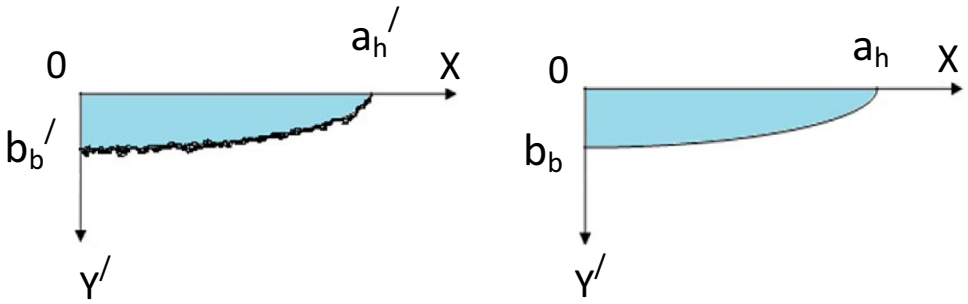

Fig. 1 The wetted area pattern which occurred depending on the simultaneous movement of water on the soil surface and in the soil profile in the furrow irrigation system

of time from the beginning of the irrigation is smaller than the water advance period in the furrow ($T_b < T_i$), water does not reach the end of the furrow in period T_b. While horizontal movement of water is continuing on the soil surface, it infiltrates into the soil in a vertical direction at the same time. Water infiltrates into the soil with a velocity of $\frac{\partial b_b}{\partial t} = i_b$ depending on the features of the soil. In the vertical movement, as the elapsed time from the beginning of the irrigation is smaller than the net infiltration period ($T_b < T_n$), the depth of water infiltrating the soil at the head of the furrow during the period T_b is smaller than the net irrigation water requirement of the crop ($b_b < D_n$) (Fig. 2). The net infiltration period (T_n) is the length of time for the infiltration of the net irrigation water requirement of the crop.

Water moves simultaneously in both vertical and horizontal directions in a blocked end furrow, creating a wetted area pattern in the soil profile. This shape is ellipsoidal, as explained previously. The size of the wetted area in the soil profile during the period T_b from the beginning of the irrigation can be determined by the following equations:

$$A_T = \frac{\pi}{4} a_h b_b \tag{1}$$

In Eq. 1, A_T: cross sectional area of the infiltration profile along the furrow during the period T_b from the beginning of the irrigation (cm^2); a_h: advance of water on the soil surface in the furrow at any time point t from the beginning of the irrigation (cm) (Fig. 2); b_b: depth of water infiltrating the soil at the head of the furrow during the period T_b from the beginning of the irrigation (cm) (Fig. 2).

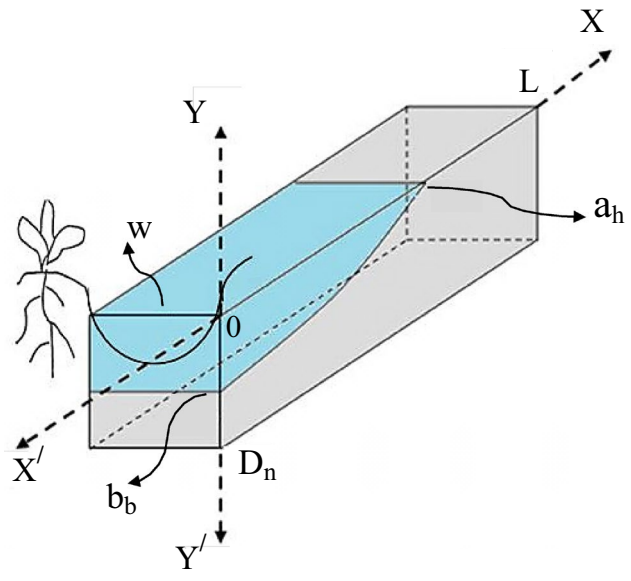

Fig. 2 Movement of water in a furrow and the wetted area pattern, when the elapsed time from the beginning of the irrigation is smaller than the water advance period ($T_b < T_i$)

As the variables on both sides of the equation are functions of time, they can be derived according to time (t).

$$\frac{\partial A_T}{\partial t} = \frac{\pi}{4}\left[\frac{\partial}{\partial a_h}(a_h)\frac{\partial a_h}{\partial t} b_b + \frac{\partial}{\partial b_b}(b_b)\frac{\partial b_b}{\partial t} a_h\right]$$

$$\Rightarrow \frac{\partial A_T}{\partial t} = \frac{\pi}{4}\left[b_b \frac{\partial a_h}{\partial t} + a_h \frac{\partial b_b}{\partial t}\right]$$

$$\frac{\partial A_T}{\partial t} = \frac{\pi}{4}\left(b_b v + a_h i_b\right)$$

$$V_{AT} = \frac{\pi}{4}\left(b_b v + a_h i_b\right) \tag{2}$$

In Formula 2, V_{AT}: rate of change of the cross sectional area of the infiltration profile along the furrow at any moment t of the irrigation ($cm^2\ h^{-1}$).

Water continues its horizontal advance in the furrow over a definite period. When the advance distance and the advance time of water between two definite points on the soil surface are measured, the horizontal advance velocity of water can be determined by the formula given below.

$$\Delta v = \frac{\Delta x}{\Delta t_a} \tag{3}$$

Δv = Horizontal advance velocity of water on the soil surface ($m\ min^{-1}$).

Δx = Distance between two definite points where water advances on the soil surface (m).

Δt_a = Advance time of water between two definite points (min).

If these processes are implemented with three repetitions and the average velocity is calculated, the value of this component refers to v ($m\ min^{-1}$).

The rate of change in the size of the wetted area in the soil profile at any moment t of the irrigation can be determined by Eq. 2 given above. The increment acceleration of this wetted area is as follows:

$$\frac{\partial^2 A_T}{\partial t^2} = \frac{\pi}{4}\left[\frac{\partial}{\partial b_b}(b_b)\frac{\partial b_b}{\partial t} v + \frac{\partial}{\partial a_h}(a_h)\frac{\partial a_h}{\partial t} i_b\right]$$

$$\Rightarrow \frac{\partial^2 A_T}{\partial t^2} = \frac{\pi}{4}\left[\frac{\partial b_b}{\partial t} v + \frac{\partial a_h}{\partial t} i_b\right]$$

$$\frac{\partial b_b}{\partial t} = i_b \text{and} \frac{\partial a_h}{\partial t} = v$$

$$\frac{\partial^2 A_T}{\partial t^2} = \frac{\pi}{4}\left[i_b v + v i_b\right] \Rightarrow \frac{\partial^2 A_T}{\partial t^2} = \frac{\pi}{4}\left(2 i_b v\right)$$

$$\frac{\partial^2 A_T}{\partial t^2} = \frac{\pi}{2} i_b v \tag{4}$$

In Eq. 4, $\partial^2 A_T/\partial t^2$: the increment acceleration of the wetted area ($cm^2\ h^{-2}$); i_b: infiltration velocity of water in soil at the head of the furrow ($cm\ h^{-1}$); v: average advance velocity of water on soil surface in a horizontal direction ($cm\ h^{-1}$).

In the next stage, while multidirectional movement of water is continuing in the furrow, a wetted area pattern also occurs in the soil profile. The border line connecting b_b and b_s can be considered as a line with a slope (Fig. 3). This is because, while the infiltration depth of water into the soil in a vertical direction has a small value, the length of the furrow might be hundreds of times greater than the infiltration depth. For example, the net irrigation water requirement of a crop was $D_n = 84.2$ mm while the length of the furrow was $L = 175$ m (Yıldırım 2013). Here, there is a nearly 2078.4 times difference between the length of the furrow and the net irrigation water requirement of the crop. Because of this, the border between b_b and b_s can be considered as a linearized line with slope (Fig. 3). Description of the curvilinear border of the infiltration pattern for every time point during the irrigation application by different nonlinear functions, which shows a continuous variation for each time point in spatio-temporal dimensions, and the running of these functions many times repeatedly for consecutive time points are very complex processes in a furrow irrigation system. Therefore, the curvilinear border of the infiltration pattern was linearized as a sloping line. This procedure enabled the model to be run for many consecutive time points in spatio-temporal dimensions. High levels of water application efficiency have been obtained by running the model for different sample applications. This solution approach has reduced the complexity of the model and the calculation intensity.

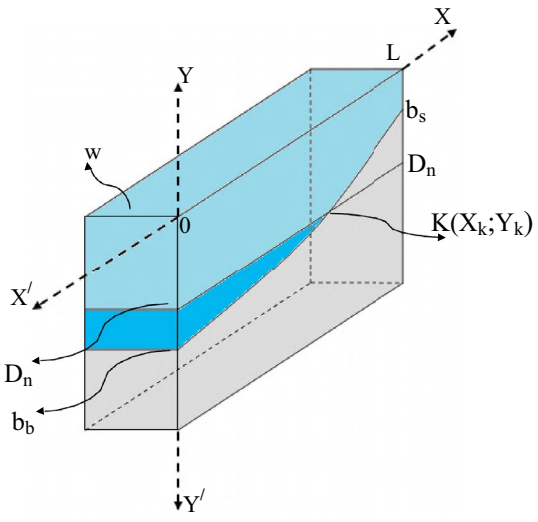

Fig. 3 Schematic description of the wetted area caused by deep percolation and the dry area which has not yet been irrigated in the soil profile, on the coordinate system

Water infiltrates the soil with a velocity of $\frac{\partial b_b}{\partial t} = i_b$ at the head of the furrow. However, as the elapsed time from the beginning of the irrigation is greater than the net infiltration period at the head of the furrow ($T_b > T_n$), the depth of water infiltrating the soil in this part of the furrow is greater than the net irrigation water requirement of the crop ($b_b > D_n$). Therefore, deep percolation with a value of ($b_b - D_n$) mm occurs at the head of the furrow. The size of the area of the right-angled triangle (b_b, D_n, K) in the soil profile shows the size of the wetted area caused by the deep percolation at any moment t of the irrigation (Fig. 3).

In Fig. 3, it is necessary to determine the coordinates of the intersection point $K(X_k;Y_k)$ of the slopeless line showing the net irrigation water requirement of the crop (D_n), and the sloping line [b_b b_s] formed by water at the border of the wetted area pattern in the soil profile. The coordinate of this intersection point K can be determined by the common solution of both the equations of these two lines. The equation of this sloping line between the points b_b and b_s was determined according to the principle of the equation of the line containing two points. The coordinates of these two points, which were on the sloping line [b_b b_s], were ($0;b_b$) and (L; b_s), respectively. Thus, the equation of the sloping line [b_b b_s] is determined as follows:

$$\frac{y - b_b}{b_b - b_s} = \frac{x - 0}{0 - L}$$

$$y - b_b = -\frac{x}{L}(b_b - b_s)$$

$$y = \frac{(b_s - b_b)}{L} x + b_b \tag{5}$$

The equation of the line without slope which shows the net irrigation water requirement of the crop in Fig. 3 is given below.

$$y = D_n$$

The coordinate of the intersection point $K(X_k; Y_k)$ of the sloping line [b_b b_s] and the slopeless line $y = D_n$ was determined by the common solution of the equations of these two lines, as explained below. First, the abscissa (X_k) of the intersection point K can be determined.

$$D_n = \frac{(b_s - b_b)}{L} x + b_b$$

$$\left(D_{\mathrm{n}}-b_b\right)=\frac{\left(b_s-b_b\right)}{L}x \tag{6}$$

Substituting X_k for X and rearranging,

$$X_k=L\frac{\left(D_{\mathrm{n}}-b_{\mathrm{b}}\right)}{\left(b_{\mathrm{s}}-b_{\mathrm{b}}\right)} \tag{7}$$

The ordinate (Y_k) of the intersection point K is determined as given below.

$$Y_k=D_{\mathrm{n}}$$

As a result, the coordinate of the point $K(X_k; Y_k)$ can be formulated as follows:

$$K\left(L\frac{\left(D_{\mathrm{n}}-b_{\mathrm{b}}\right)}{\left(b_{\mathrm{s}}-b_{\mathrm{b}}\right)};D_{\mathrm{n}}\right) \tag{8}$$

In Formula 8, K: the (coordinates of the) intersection point of the slopeless line showing the net irrigation water requirement of the crop (D_{n}), and the sloping line [b_{b} b_{s}] formed by water at the border of the wetted area pattern in the soil profile (Fig. 3); L: length of furrow (cm); D_{n}: net irrigation water requirement of the crop in any irrigation period (cm); b_{b}: Depth of water infiltrating the soil at the head of the furrow during the period T_{b} from the beginning of the irrigation (cm); b_{s}: depth of water infiltrating the soil at the end of the furrow during the infiltration period T_{s} (cm).

In this stage, the wetted area pattern in the soil profile at any moment t of the irrigation is a right-angled trapezoid with corner points 0, b_{b}, b_{s} and L (Fig. 3). Therefore, the size of the wetted area is determined as follows:

$$A_{\mathrm{T}}=\frac{L}{2}\left(b_{\mathrm{b}}+b_{\mathrm{s}}\right). \tag{9}$$

In this stage, the rate of change in the size of the wetted area at moment t of the irrigation can be determined as follows:

$$\frac{\partial A_{\mathrm{T}}}{\partial t}=\frac{L}{2}\left(i_{\mathrm{b}}+i_{\mathrm{s}}\right)$$

$$V_{\mathrm{AT}}=\frac{L}{2}\left(i_{\mathrm{b}}+i_{\mathrm{s}}\right). \tag{10}$$

In the formula above, V_{AT}: rate of change of the size of the wetted area in the soil profile at any moment t of the irrigation ($\mathrm{cm}^2\ \mathrm{h}^{-1}$); L: length of furrow (cm); i_{b}: infiltration velocity of water in the soil at the head of the furrow (cm h^{-1}); i_{s}: infiltration velocity of water in the soil at the end of the furrow (cm h^{-1}).

The size of the wetted area caused by deep percolation at any moment t in this stage of the irrigation is equal to the area of the right-angled triangle (A_1) with corner points b_{b}, D_{n} and K (Fig. 3). Also in this process, the size of the dry area which has not yet been irrigated in the soil profile at moment t of the irrigation is equal to the area of the right-angled triangle (A_2) whose corner points are b_{s}, D_{n} and K (Fig. 3).

The size of the wetted area (A_1) caused by deep percolation from the head of the furrow in the soil profile at moment t of the irrigation can be formulated as follows (Fig. 3):

$$Z_{\mathrm{b}}=\left(b_{\mathrm{b}}-D_{\mathrm{n}}\right) \tag{11}$$

$$A_1=\frac{Z_{\mathrm{b}}}{2}X_k. \tag{12}$$

When the value of X_k is inserted in this formula, the following equation is obtained:

$$A_1=\frac{Z_{\mathrm{b}}}{2}\frac{L\left(D_{\mathrm{n}}-b_{\mathrm{b}}\right)}{\left(b_{\mathrm{s}}-b_{\mathrm{b}}\right)}\Rightarrow A_1=\frac{Z_{\mathrm{b}}}{2}\frac{L\left(-Z_{\mathrm{b}}\right)}{\left(b_{\mathrm{s}}-b_{\mathrm{b}}\right)}$$

$$A_1=\frac{-Z_{\mathrm{b}}^2L}{-2(b_{\mathrm{b}}-b_{\mathrm{s}})}$$

$$A_1=\frac{Z_{\mathrm{b}}^2L}{2(b_{\mathrm{b}}-b_{\mathrm{s}})}. \tag{13}$$

In Eq. 13, A_1: the size of the wetted area caused by deep percolation at moment t of the irrigation application (cm^2) (Fig. 3). $Z_{\mathrm{b}}=(b_{\mathrm{b}}-D_{\mathrm{n}})$. L: length of furrow (cm). D_{n}: net irrigation water requirement of the crop in any irrigation period (cm). b_{b}: depth of water infiltrating the soil at the head of the furrow during the period T_{b} from the beginning of the irrigation (cm). b_{s}: depth of water infiltrating the soil at the end of the furrow during the infiltration period T_{s} (cm).

As the infiltration period at the end of the furrow is smaller than the net infiltration period ($T_{\mathrm{s}}<T_{\mathrm{n}}$), the depth of water infiltrating the soil in this part of the furrow is less than the net irrigation water requirement of the crop ($b_{\mathrm{s}}<D_{\mathrm{n}}$). In other words, there is a dry area which has not yet been irrigated in the soil profile at the end of the furrow (Fig. 3). The size of the area (A_2) remaining dry in the soil profile at moment t of the irrigation can be formulated as shown below. Area A_2 is the right-angled triangle whose the corner points are b_{s}, D_{n} and K, as seen in Fig. 3:

$$Z_{\mathrm{s}}=\left(D_{\mathrm{n}}-b_{\mathrm{s}}\right) \tag{14}$$

$$A_2 = \frac{Z_s}{2}\left(L - X_k\right). \tag{15}$$

The equation given below is obtained when the value of X_k is inserted in the formula above for moment t of the irrigation.

$$A_2 = \frac{Z_s}{2}\left(L - \frac{L\left(D_n - b_b\right)}{\left(b_s - b_b\right)}\right) \Rightarrow A_2 = \frac{Z_s L}{2}\left(1 - \frac{\left(D_n - b_b\right)}{\left(b_s - b_b\right)}\right)$$

$$A_2 = \frac{Z_s L}{2}\left(1 - \frac{-\left(b_b - D_n\right)}{-\left(b_b - b_s\right)}\right) \Rightarrow A_2 = \frac{Z_s L}{2}\left(1 - \frac{\left(b_b - D_n\right)}{\left(b_b - b_s\right)}\right)$$

$$Z_b = \left(b_b - D_n\right) \tag{11}$$

$$A_2 = \frac{Z_s L}{2}\left(1 - \frac{Z_b}{\left(b_b - b_s\right)}\right)$$

The formula of A_2 above can be arranged as shown below by Eqs. 11 and 14.

$$b_b - b_s = Z_b + Z_s$$

$$A_2 = \frac{Z_s L}{2}\left(1 - \frac{Z_b}{Z_b + Z_s}\right) \tag{16}$$

In Eq. 16, A_2: the size of the dry area which has not yet been irrigated in the soil profile at moment t of the irrigation application (cm^2) (Fig. 3); $Z_b = (b_b - D_n)$ and $Z_s = (D_n - b_s)$, L: length of furrow (cm); b_b: depth of water infiltrating the soil at the head of the furrow during the period T_b from the beginning of the irrigation (cm); b_s: depth of water infiltrating the soil at the end of the furrow during the infiltration period T_s (cm); D_n: net irrigation water requirement of the crop in any irrigation period (cm).

The first of the two indices which are very important in this stage of the irrigation is that as the elapsed time from the beginning of the irrigation (T_b) increases, the size of the area A_1 also increases, and at the same time the area A_2 decreases. The size of the area A_2 takes the value zero when the infiltration period at the end of the furrow is equal to the net infiltration period ($T_s = T_n$), and because in this, no dry area without irrigation will remain in the soil profile in the furrow. The second index is that as the length of the elapsed time (T_b) from the beginning of the irrigation increases, the value of abscissa X_k also increases. Also, when the infiltration period at the end of the furrow is equal to the net infiltration period ($T_s = T_n$), the value of X_k will be equal to the length of the furrow L. In other words, when D_n mm of water infiltrates the soil at the end of the furrow, the value of X_k must be equal to the length of the furrow (L) because the desired amount of water (D_n) will have been delivered to the end of the furrow in this condition. These two main indices constitute the references in verifying the validity of the devised model.

In addition, Christiansen's uniformity coefficient (CU) is used to evaluate the irrigation water distribution uniformity in the soil along the furrow length (Wu et al. 2017) as follows:

$$\mathrm{CU} = \left(1 - \left(\sum \left|X_i - X_m\right|\right) \Big/ \sum X_i\right) \times 100, \tag{17}$$

where X_i = amount of water which infiltrated the soil at the head and end of the furrow during the elapsed time from the beginning of the irrigation (mm).

X_m = average depth of water which infiltrated the soil during the elapsed time from the beginning of the irrigation (mm).

Christiansen's uniformity coefficient is calculated in accordance with the amount of water which infiltrates the soil at the head and end of the furrow during the elapsed time from the beginning of the irrigation and is given for the sample application in the paper and in the Supplementary Materials.

Sample application for the blocked end furrow irrigation system

The proposed model was run for the sample application of the blocked end furrow system, which was published previously by Yıldırım (2013). Water conveyance and distribution were performed by open canal system. The plot where the blocked end furrow system was designed was in the shape of a rectangle without slope and was (250 × 350) m in size. Also, the blocked end furrow had no slope in the irrigation direction, and the water advanced along the furrow by means of the hydraulic slope. The water source discharge was $Q = 80$ L s^{-1}, and the maximum inflow to each furrow was $q_{max} = 1.4$ L s^{-1}. The crop was maize, and the distance between rows was 70 cm. The net irrigation water requirement of the crop was 84.2 mm, and irrigation could be performed 24 h a day. The infiltration test for the furrow was carried out according to the inflow–outflow method. It was determined that the soil type was in the I_f 0.40 infiltration group according to the USDA-SCS criteria (Yıldırım 2013; USDA SCS 2012).

Solution process for the sample application by the USDA SCS method

The blocked end furrow system design was carried out in line with these data as explained by Yıldırım (2013) as follows;

The soil where the blocked end furrow system was designed was in the I_f 0.40 infiltration group according to the USDA-SCS criteria. The values of the coefficients for this group were $a = 1.064$, $b = 0.736$, $c = 7.0$, $f = 7.79$ and $g = 2.23 \times 10^{-4}$.

In this way, the infiltration equation was represented by the formula $D = aT^b + c$ (USDA SCS 2012; Yıldırım 2013). When the coefficients were inserted in the equation, $D = 1.064T^{0.736} + 7$ was obtained.

Distance between furrows

Distance between rows for the maize was 70 cm. As this value was greater than 50 cm, one furrow was prepared for each crop row, and the distance between furrows was taken to be $w = 0.70$ m.

3. The maximum number of furrow sets across the width of the plot

The system discharge and the maximum inflow to the furrows were $Q = 80$ L s^{-1} and $q_{max} = 1.4$ L s^{-1}, respectively. In these conditions, the minimum number of furrows in a furrow set was

$$n_{min} = \frac{Q}{q_{max}} = \frac{80}{1.4} = 57$$

Under these conditions, the minimum width of one furrow set was

$$b_{min} = wn_{min} = 0.70 \times 57 = 40\text{m}$$

The maximum number of furrow sets which can be placed across the width of the plot was

$$N_{max} = \frac{250}{40} = 6$$

Suitable furrow length and inflow to the furrow

Four alternative solutions were obtained by Yıldırım (2013) in designing this blocked end furrow system, as follows:

Alternative I

The results for the alternative solution I are given in Table 1.

According to these results, as the values were $T_i = 154$ 9 min $> 0.60 \times T_n = 221$ min, a furrow length of $L = 350$ m was not suitable.

In this way, six sets of furrows were placed across the width of the plot, and the solution process was carried out again for a furrow length of $L = 175$ m (=350/2) and an inflow to the furrow of $q = 1.33$ L s^{-1}. The results obtained are as follows:

As the values were $T_i = 78$ min $< 0.60 \times T_n = 254$ min, a furrow length of $L = 175$ m was suitable.

The data for the four alternative solutions are given in Table 2 (Yıldırım 2013).

In these solutions, a furrow length of $L = 175$ m was found to be suitable according to alternatives I, II and III.

Table 1 The results for the alternative solution I

Components of the furrow system	Results for alternative I	Components of the furrow system	Results for alternative I
Number of furrow sets in the width of the plot (N_{max})	6	Wetted perimeter (P) (m)	0.66
Inflow to the furrow (q) (L s^{-1})	1.33	Net infiltration period (T_n) (min)	368
Length of furrow (L) (m)	350	Water advance period (T_i) (min)	1549
Average hydraulic slope (S_0) (m m^{-1})	0.00028		

Table 2 The data for the four alternative solutions

Alternatives	I	II	III	IV
Number of furrow sets in the width of the plot	6	5	4	3
Length of furrow (L) (m)	175	175	175	175
Inflow to the furrow (q) (L s^{-1})	1.33	1.13	0.90	0.67
Water advance period (T_i) (min)	78	102	163	362
Net infiltration period (T_n) (min)	423	445	481	521
$0.60 \times T_n$	254	267	289	313
Comparison of the T_i and $0.60 \times T_n$	$T_i < 0.60 \times T_n$	$T_i < 0.60 \times T_n$	$\boldsymbol{T_i < 0.60 \times T_n}$	$T_i > 0.60 \times T_n$

However, in alternative IV, as the values were $T_i = 362$ min $> 0.60 \times T_n = 313$ min, a furrow length of $L = 175$ m was found not to be suitable. As the lowest flow rate of the furrow was found in alternative III, this choice was taken into consideration in planning the system.

Solution process for alternative III

The solution process was carried out for four sets of furrows, placed across the width of the plot, length of furrow $L = 175$ m and the inflow to the furrow $q = 0.90$ L s^{-1}. The calculations for alternative III are given below (Yıldırım 2013).

– The maximum number of furrow sets which could be placed across the width of the plot:

The system discharge and the inflow to the furrow were $Q = 80$ L s^{-1} and $q = 0.90$ L s^{-1}, respectively. The results for the alternative solution III are given in Table 3.

The same problem was also solved by the method which was newly devised in this investigation. Features of flow occurring in the blocked end furrow system and movement of water in soil were described by separating them into stages, and results were obtained.

Application of the new method for the design of the furrow irrigation system

Movement equations of water both on the soil surface and in the soil profile, time-dependent function of the wetted area pattern, relative velocities of the components of the furrow irrigation system and deep percolation equations, which were devised in this investigation, were applied to the solution of the furrow irrigation problem published previously by Yıldırım (2013). The model was run for alternative III, the components of which were four sets of furrows, placed across the width of the plot and the inflow to the furrow $q = 0.90$ L s^{-1}. The length of the furrow was determined according to the new method.

As stated previously, the equation of the net infiltration period for the blocked end furrow system is as given below (USDA SCS 2012; Yıldırım 2013).

$$T_n = \left(\frac{d_n \frac{w}{P} - c}{a} \right)^{1/b} \tag{18}$$

When this equation is rearranged, it takes the following form:

$$d_n = \left(a T_n^b + c \right) \frac{P}{w}.$$

When the values of the coefficients are written in the equation above, the amount of water infiltrating the soil in any particular zone of the furrow at any moment T of the irrigation can be found as depth of water (d) by means of the following formula (USDA SCS 2012; Yıldırım 2013):

$$d = \left(a T^b + c \right) \frac{P}{w}. \tag{19}$$

In Eq. 19, d: the amount of water infiltrating the soil at any moment T of the irrigation (mm); T: any time point from the beginning of the irrigation application (min); w: distance between two furrows (m); P: wetted perimeter of the furrow (m); a, b, c: coefficients for the soil type according to the USDA-SCS infiltration groups.

$$d = \left(1.064 \times T^{0.736} + 7.0 \right) \frac{0.55}{0.70}$$

Also, the infiltration velocity in a particular zone of the furrow at any moment T of the irrigation was found by the derivative of Eq. 19 according to time. When this process was carried out, the following formula was obtained:

$$I = \left(\frac{P}{w} \right) a b T^{b-1}. \tag{20}$$

In Eq. 20, the variable I represents the infiltration velocity (mm min^{-1}). The units of the other variables in this equation are the same as the ones in Eq. 19.

Table 3 The results for the alternative solution III

Components of the furrow system	Results for alternative III	Components of the furrow system	Results for alternative III
Number of furrow sets in the width of the plot (N_{max})	4	Water advance period (T_i) (min)	163
Inflow to the furrow (q) (L s^{-1})	0.90	Average infiltration period (T_0) (min)	527
Length of furrow (L) (m)	175	Length of irrigation time (T_a) (min)	204
Average hydraulic slope (S_0) (m m^{-1})	0.00048	Total amount of water to be applied (d_t) (mm)	89.9
Wetted perimeter (P) (m)	0.55	Amount of deep percolation (d_s) (mm)	5.7
Net infiltration period (T_n) (min)	481	Water application efficiency (E_a) (%)	93.7

In Eq. 20, the infiltration velocity in a particular zone of the furrow was found in mm min^{-1} at any moment T of the irrigation. The variables of i_b and i_s in the new model are calculated in accordance with the formula below. When the values of the coefficients were inserted into the equation of the infiltration velocity, the formula took the following form: $I = \left(\frac{0.55}{0.70}\right) \times 1.064 \times 0.736 \times T^{(0.736-1)}$

The infiltration velocity was determined as a consecutive calculation series for each 20-min period in the model solution.

Model results

The velocity and acceleration values of the main variables of the furrow irrigation system were determined, and their variations in spatio-temporal dimensions were investigated.

Time-dependent variations of the velocity of the infiltration at the head of the furrow and rate of change of the cross-sectional area of the infiltration profile are shown in Fig. 4.

Water both moved horizontally in the flow direction and infiltrated the soil profile in the furrow during the period from the beginning of the irrigation to the 163rd minute. This movement of water in two directions occurs simultaneously. Water reached the end of the furrow in the 163rd minute. This length of time represents the water advance period (T_i) in the furrow.

The infiltration velocity has a smaller value at a given time point from the beginning of the irrigation in the parts of the furrow which have been in contact with the water for a longer time, but greater when the contact time is shorter (Fig. 5). For instance, as seen in Fig. 5, at time point t_4, infiltration velocity at point E is the highest, and infiltration velocities at points D, C, B and A follow it, respectively, from higher to lower values. As water covered the soil for a longer period at the head of the furrow, the pores contain more water than the ones at the middle and end parts of the furrow. Therefore, the infiltration velocity

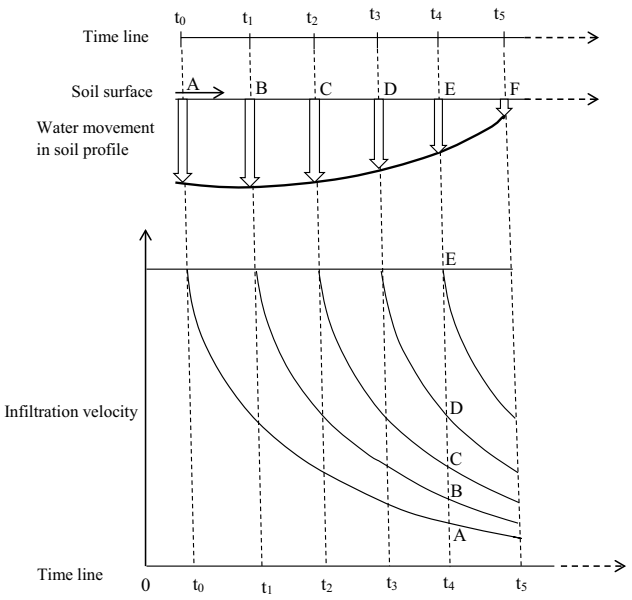

Fig. 5 Schematic description of simultaneous movement of water both on soil surface and in soil profile, and infiltration velocity at different time points in furrow irrigation system

at the head of the furrow showed a decreasing trend according to time (Fig. 4). Apart from this, the depth of water infiltrating the soil profile at the head of the furrow is also greater than that in the middle and end parts of the furrow (Fig. 5). In addition, water moves from the head of the furrow where soil pores contain more water to the middle and end parts of the furrow where the pores contain less water. Because of this, the infiltration velocity at the head of the furrow is lower than the infiltration velocities of the middle and end parts of the furrow in the same period of time (Fig. 5).

In this process, horizontal movement of water on the soil surface is speedier than the movement by infiltration in the soil profile. Apart from this, as seen in Fig. 4, the decrease

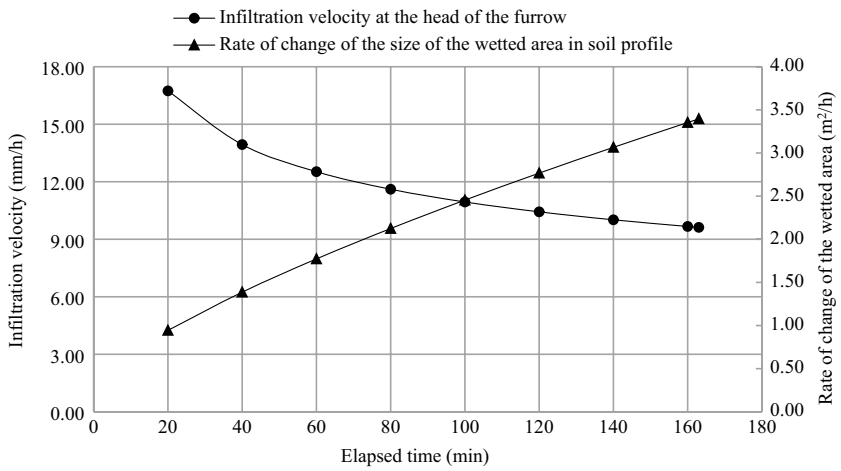

Fig. 4 Time-dependent variations of the infiltration velocity at the head of the furrow and rate of change of the cross sectional area of the infiltration pattern

in infiltration velocity depending on time at the head of the furrow also affects the horizontal movement of water on the soil surface.

The size of the wetted area in the soil profile also increased depending on the advance of water on the soil surface. As seen in Fig. 4, the wetted area in the soil profile showed an increase which slowed over time. However, the decrease in increment rate of the size of the wetted area was smaller than the decrease in infiltration velocity. The reason was that water moves from the zones in which pores contain more water to the zones in which pores contain relatively little water. This can be seen in detail in Fig. 6, which shows the variation of acceleration of the size of the wetted area.

Rate of change and acceleration of increase of the size of the wetted area in the soil profile are shown in Fig. 6.

As seen in Fig. 6, the size of the wetted area in the soil profile showed an increase which slowed over time. In other words, the wetted area was getting bigger at a decreasing rate. The most important reason was that infiltration velocity decreases depending on time. As water was infiltrating the soil at a decreasing rate, the rate of increase in the size of the wetted area also decreased. As seen in Fig. 6, a decreasing trend of acceleration of the wetted area indicated that the rate of increase of the size of the wetted area was decreasing. The results obtained from the devised model showed a similar trend to the movement of water in the soil.

In the next stage of the irrigation, deep percolation began from the head of the furrow to the end, depending on time (Fig. 3). When the net irrigation water requirement of the crop was met at the head of the furrow, the dry area in the soil profile was irrigated at the middle and end parts of the furrow. The temporal variation of the value of the abscissa

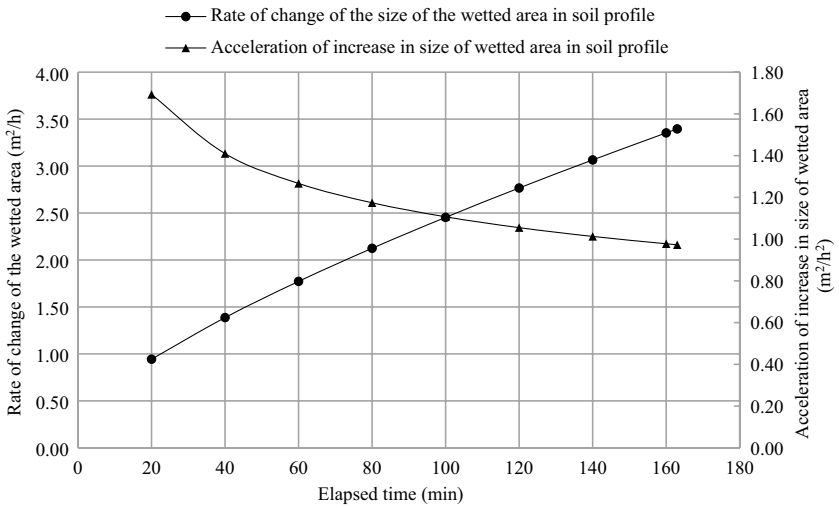

Fig. 6 Rate of change and acceleration of increase in size of wetted area in soil profile

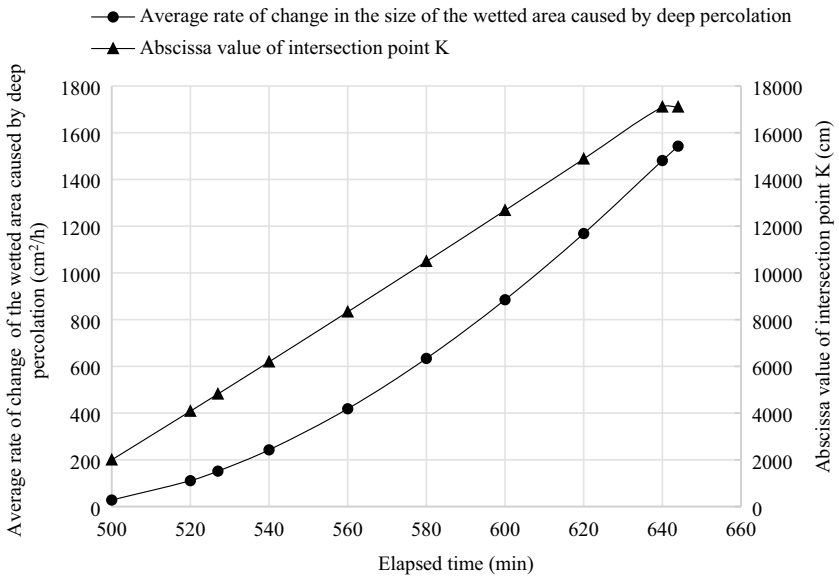

Fig. 7 Abscissa value of intersection point $K(X_k; Y_k)$ and average rate of change in the size of the wetted area caused by deep percolation, depending on time

of the intersection point $K(X_k; Y_k)$ given in Fig. 3 and average rate of change in the size of the wetted area caused by deep percolation are given in Fig. 7.

As seen in Fig. 3, the amount of water which infiltrated the soil at the head of the furrow was greater than the net irrigation water requirement of the crop, i.e. deep percolation was occurring. On the other hand, the net irrigation water requirement of the crop had not yet been met at the middle and end parts of the furrow. In this process, deep percolation was increasing depending on time from the head of the furrow to the middle and end parts.

As seen in Fig. 3, while the size of the wetted area remaining on the left side of the intersection point *K*, and which was caused by deep percolation, was showing an increment in time, the dry area on the right side of the point *K* was decreasing.

As seen in Fig. 7, the average rate of change in the size of the wetted area from deep percolation increased gradually from 27.92 to 1542.53 $cm^2\ h^{-1}$ between the 500th and 644th minutes. At this stage of the irrigation, the average rate of change in the size of the wetted area caused by deep percolation was 27.92 $cm^2\ h^{-1}$ in the 500th minute of the irrigation application. The reason for this was that the amount of water which infiltrated the soil at the head of the furrow in the 481th minute of the irrigation was equal to 84.2 mm, which was the net irrigation water requirement of the crop, i.e. the net irrigation water requirement of the crop was met at the head of the furrow in the 481st minute of the irrigation. On the other hand, this amount of water had not yet infiltrated the soil at the middle and end parts of the furrow. Because of this, while deep percolation was occurring at the head of the furrow in this period, infiltration was also continuing in the middle and end parts of the furrow in order to meet the net irrigation water requirement of the crop. In this process, deep percolation was also occurring at the head of the furrow during the period of 19 min between the 481st and 500th minutes of the irrigation application. Therefore, the average rate of change in size of the wetted area from deep percolation took the value of 27.92 $cm^2\ h^{-1}$ in the 500th minute of the irrigation (Fig. 7). At the same time, the horizontal distance (the abscissa value of intersection point *K*) where deep percolation occurred along the length of furrow also showed an increment depending on time, and at the end of this process this distance reached the value of 171.02 m along the furrow in the (163 + 481 =) 644th minute of the irrigation (Fig. 7). According to the model solution, the value of 171.02 m (the abscissa value of intersection point K) was found to be 2.27% shorter than the length of the furrow (175.00 m) determined according to the USDA SCS method given by Yıldırım (2013). The amount of water which infiltrated the soil at that moment was 84.2 mm, which was the net irrigation water requirement of the crop for this irrigation period.

The results above were found by means of the calculation process given below. Water infiltrated the soil at the head of the furrow during a period of 163 + 481 = 644 min from the beginning of the irrigation. The amount of water infiltrating the soil at the head of the furrow was determined by the Eq. 19.

When the values of the coefficients were written in the Eq. 19 and the solution was found for $T = 644$ min, the amount of water which infiltrated the soil at the head of the furrow (b_b) was obtained as 103.1 mm.

At the end of the furrow, water infiltrated the soil during the net infiltration period (T_n) of 481 min. During this period, the amount of water infiltrating the soil at the end of the furrow must be equal to the net irrigation water requirement of the crop (84.2 mm). Also, when the calculation process was carried out using the infiltration equation given above (Eq. 19) for $T = 481$ min, the amount of water which infiltrated the soil at the end of the furrow (b_s) was obtained as 84.2 mm.

Therefore, no dry area which had not yet been irrigated remained in the soil profile at the end of the furrow. Thus, the size of the A_2 area calculated by Eq. 16 took the value of zero.

According to the model solution, the length of the furrow (the abscissa value of intersection point *K*) was determined as 171.02 m, where 84.2 mm of water (the net irrigation water requirement of the crop) infiltrated the soil at the end of the furrow (Figs. 7, 8). Also, the net infiltration period (T_n) was 481 min, and the water advance period (T_i) was 163 min. Therefore, the size of the dry area (A_2) which had not yet been irrigated took the value zero. When the model was run according to these data, an analysis could be made of how close the value of A_2 was to zero.

In order to evaluate the results in more detail, the value of $b_s = 84.2$ mm, which was determined above, was taken as $b_s = 84.19$ mm in the equation of A_2 (Eq. 16). Otherwise, if the values were taken as $b_s = D_n = 84.2$ mm for the end of the furrow, the value of Z_s (Eq. 14) would be equal to zero ($Z_s = D_n - b_s = 0$), and also the solution of Eq. 16 would be found to be zero. Because of this, the value of $L = 171.02$ m (the abscissa value of intersection point *K*) which was obtained from the model solution could not be analyzed in this state. This was the reason why the value of b_s was taken as 84.19 mm in Eq. 16. The proposed model is verified by running the Eq. 16. The data and the results are given in Table 4.

As the value of the size of the A_2 area was very close to zero, it is possible to reach the conclusion that no dry unirrigated area remained in the soil profile at the end of the furrow.

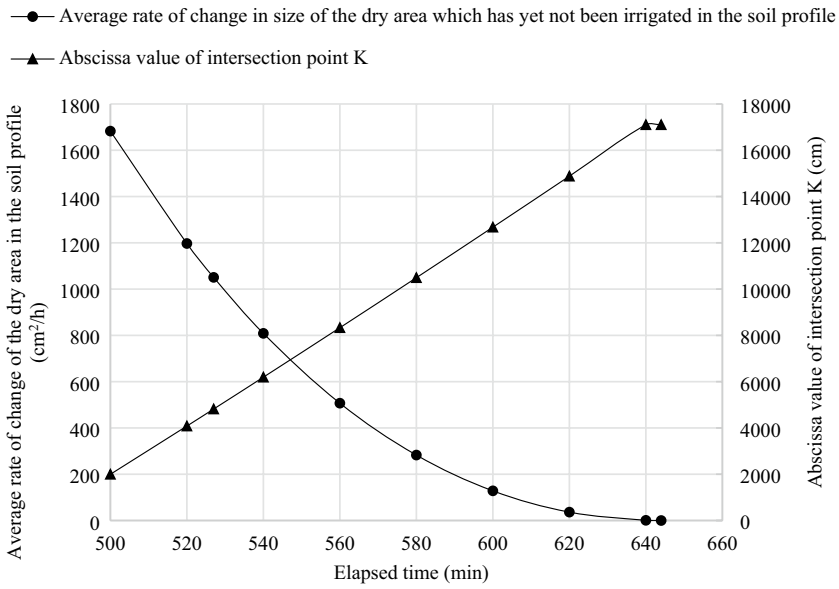

Fig. 8 Time-dependent variation of both the average rate of change in size of the dry area which has yet not been irrigated in the soil profile and abscissa values of the intersection point *K*.

Table 4 Verification of the model results

Components of the wetting pattern	Values of the components	Components of the wetting pattern	Values of the components
b_b (cm)	10.31	$Z_b = b_b - D_n$ (cm)	1.89
b_s (cm)	8.419	$Z_s = D_n - b_s$ (cm)	0.001
D_n (cm)	8.42	$Z_b + Z_S$ (cm)	1.891
L (cm)	17,102	A_2 (cm^2)	0.0045

In this process, an increment in both the horizontal distance where deep percolation occurred and the average rate of change in size of the wetted area from deep percolation showed that the devised model gave results suitable to the movement of water in soil.

Time-dependent variation of both the average rate of change in size of the dry area which had not yet been irrigated in the soil profile and the abscissa values of the intersection point *K* are given in Fig. 8.

This process continued until the net irrigation water requirement of the crop was met at the end of the furrow. Deep percolation occurred at the head of the furrow over a period of 19 min in the 500th minute of the irrigation. At this moment, the average rate of change in the size of the dry area which has not yet been irrigated in the soil profile was 1682.71 cm^2 h^{-1}. As seen in Fig. 8, this value decreased gradually until the 644th minute of the irrigation, when it took the value of 0.0 cm^2 h^{-1}. As a result, the average rate of change in size of the dry area which had not yet been irrigated decreased gradually from the 500th minute of the irrigation to the 644th minute. Also, irrigation was completed when 84.2 mm net irrigation water requirement had infiltrated the soil at the end of the furrow. These results from the model solution described suitably the movement of water in the soil profile in spatio-temporal dimensions.

In this stage, the gradual increment in the average rate of change in the wetted area caused by deep percolation in the soil profile and at the same time the gradual decrease in the average rate of change in the dry area which had yet not been irrigated are given as a graph in Fig. 9.

In this process, as the amount of deep percolation at the head of the furrow increased towards the middle and end parts of the furrow, the size of the dry area which had not yet been irrigated in the soil profile decreased depending on time, and took the value of zero at the end of the furrow. As seen in Fig. 3, the three variables which showed a simultaneous variation in the soil profile depending on the movement of water—average rates of change in the wetted area by deep percolation and the dry area which had not yet been irrigated in the soil profile, and the length of the furrow which was being reached by the movement of water in the soil—showed a trend which accorded with the results from the model solution.

In addition, the water distribution uniformity (CU) along the furrow was determined by Christiansen's uniformity coefficient.

$X_1 = b_b = 103.1$ mm.

$X_2 = b_s = 84.2$ mm.

$X_m = 93.65$ mm.

CU = 89.9% ≅ 90%

Water distribution uniformity of 90% is classified in the "good" category (Piazentin et al. 2019). Minimization of deep percolation in the proposed model also minimizes the difference between the amounts of water which infiltrate the

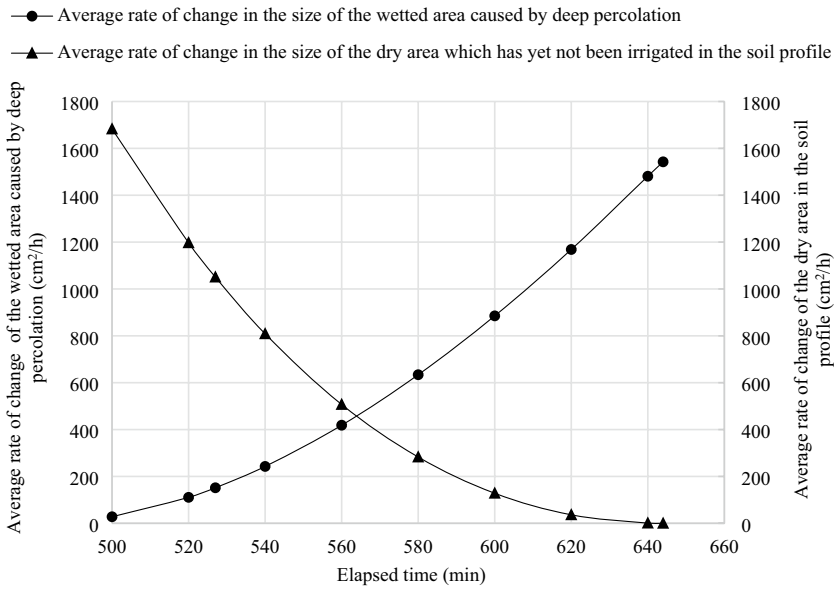

Fig. 9 Graphical view of the gradual increment of the average rate of change in the wetted area caused by deep percolation in the soil profile, and at the same time the gradual decrease in the average rate of change in the dry area which has not yet been irrigated

soil at the head and end of the furrow. This enables the water distribution uniformity along the furrow to take high values.

Verification of the model results according to the USDA SCS method

The model results for the given crop and soil conditions indicated that the optimum length of furrow is $L = 171.02$ m, when the inflow to the furrow is $q = 0.90$ L s^{-1}, the net irrigation water requirement of the crop is 84.2 mm, and the number of furrow sets across the width of the plot is four. This length of furrow was found to be 2.27% shorter than the furrow length of 175 m given in the solution of Yıldırım (2013). The calculation process for the comparative checking and verification of the new model results was carried out in accordance with the USDA SCS method given in the Sect. 3.1 Solution Process for the Sample Application.

1) The soil type was in the I_f 0.40 infiltration group according to the USDA-SCS criteria. The values of the coefficients for this group were $a = 1.064$, $b = 0.736$, $c = 7.0$, $f = 7.79$ and $g = 2.23 \times 10^{-4}$.

   Thus, the infiltration equation was $D = 1.064T^{0.736} + 7$.

2) Distance between furrows was $w = 0.70$ m.
3) The maximum number of furrow sets which could be placed across the width of the plot.

The system discharge and the inflow to the furrow were $Q = 80$ L s^{-1} and $q = 0.90$ L s^{-1}, respectively. Results of the verification process of the proposed model according to the USDA SCS method are given in Table 5.

The model results indicated that the most suitable length of furrow was $L = 171.02$ m for the 84.2 mm net irrigation water requirement of the crop and the $q = 0.90$ L s^{-1} flow rate of furrows for the given crop and soil conditions. Under these conditions, while the water application efficiency was found to be 93.7% for the 175-m length of furrow according to the USDA SCS method (Yıldırım

Table 5 Verification of the model results according to the USDA SCS method

Components of the furrow system	Values of the components	Components of the furrow system	Values of the components
Number of furrow sets in the width of the plot (N_{max})	4	Water advance period (T_i) (min)	148.25
Inflow to the furrow (q) (L s^{-1})	0.90	Average infiltration period (T_0) (min)	520.97
Length of furrow (L) (m)	171.02	Length of irrigation time (T_a) (min)	198.06
Average hydraulic slope (S_0) (m m^{-1})	0.000494	Total amount of water to be applied (d_t) (mm)	89.3
Wetted perimeter (P) (m)	0.552	Amount of deep percolation (d_s) (mm)	5.1
Net infiltration period (T_n) (min)	478.03	Water application efficiency (E_a) (%)	94.29

2013), the water application efficiency increased to 94.29% for a 171.02 m furrow length according to the method devised in this investigation.

As a result, a high rate of water application efficiency was reached by suitable planning in the blocked end furrow system. If the topographic conditions are suitable for land levelling the blocked end furrow system has preferable features.

Discussion

Kermani et al. (2019) carried out an investigation for the estimation of water advance distance for a specific inflow in the furrow irrigation method. Thus, they tried to predict the volume of water which infiltrated the soil, and thereby it was aimed to prevent water loss and to increase water application efficiency. The Adaptive Neuro Fuzzy Inference System (ANFIS) data-driven method gave the best result. In this process, only the water advance distance was estimated. In the present investigation, simultaneous movement properties of water both on the soil surface and in the soil profile are described mathematically. The equations obtained are described as the functions of time. Thus, the most suitable combination was provided of all the parameters and the variables which affect the optimum design of the system. These procedures were carried out based on the analytical solution method, not by the trial and error approach, a numerical solution or the data-driven methods. The results provided the optimum cut-off time and furrow length, minimum deep percolation, maximum water application efficiency (94.29% and 94.18%) and a high level of water distribution uniformity (90% and 91.3%). These results indicate that the proposed method can be used in the design of a blocked end furrow system.

Nie et al. (2018) revealed that the water advance in the blocked end furrow and the water application performance indicators were not sensitive to the variations in the Manning's roughness coefficient. These results are similar to the results of Smith et al. (2018), Salahou et al. (2018) and Nie et al. (2014). The Manning's roughness coefficient showed a variation between the values of 0.038 and 0.186 for a field of maize (Nie et al. 2018). The inflow rate in the blocked end furrow was determined using Manning's roughness coefficient and the field average infiltration parameters. Apart from this, the optimal inflow rate was determined using different combinations of the various furrow lengths and bottom slope values. The inflow rates which were determined by the two different approaches were consistent with each other. In the proposed method, optimum solutions can be obtained for each desired inflow under existing irrigation condition. The optimum result is obtained from the proposed model by taking into consideration simultaneously all the parameters and the variables which affect the design of a furrow system and running them interactively within the model solution procedure. Thus, the optimum furrow length and the cut-off time are obtained which minimize deep percolation, maximize the water application efficiency (94.29% and 94.18%), and provide maximum level of water distribution uniformity (90% and 91.3%) in the soil profile. These results indicate that the model proposed can be used in the design of a blocked end furrow system.

Mazarei et al. (2021) investigated the temporal variability of the infiltration and the Manning's roughness coefficient. In addition, they studied the effects of different inflow rates on furrow irrigation performance. It was determined that when the inflow rates were increased from 1.0 to 1.5 and 2 L s^{-1}, the average values of water application efficiency were reduced at rates of 3.43% and 24.55% respectively. These results are compatible with the results of Xu et al. (2019) and Mazarei et al. (2020). Deep percolation decreased by 27.34% and 34.17% when the inflow rate was increased from 1.0 to 1.5 and 2.0 L s^{-1}. An inverse relation occurred between the inflow and the deep percolation. Water distribution uniformity in the soil profile increased by 9.7% and 9.3% for the same increment in inflow rate as was stated above. Sayari et al. (2017), Nie et al. (2019) and Mazarei et al. (2020) reported similar results. In addition, it was indicated that the cut-off time and volume of water which infiltrated the soil were significantly affected by the temporal variation of infiltration parameters and the roughness coefficient. Apart from this, results showed that an increment in inflow rate increased the cumulative rate of infiltration. These results indicate how the temporal variation of different parameters which have an effect on the design of furrow irrigation systems affect the infiltration rate, the water application efficiency, the water distribution uniformity and the deep percolation. All of these results were determined by the trial and error approach during the irrigation applications. The present investigation aims at an optimum combination of all the parameters and variables which affect the design of a furrow irrigation system. This process was carried out by the analytical solution method, not the trial and error approach. Thus, the optimum cut-off time and the furrow length were obtained, which minimize deep percolation, maximize the cross sectional area of the wetting pattern in the root zone where the net irrigation water requirement of the crop is met completely, and provide a high level of water application efficiency (94.29% and 94.18%) and water distribution uniformity (90% and 91.3%) in the soil profile. These results indicate that the proposed model can be used in the design of a blocked end furrow system.

Dialameh et al. (2018) determined that when the water head was increased from 5 to 10 cm in a conventional furrow irrigation (CFI), the amount of average cumulative infiltration increased by 92% and 102%, respectively, for 4- and

9-day irrigation intervals. Similarly, the increment in the water head in alternate furrow irrigation (AFI) increased the mean cumulative infiltration at a rate of 96% and 106%, respectively, for the same irrigation conditions given above. In this process, the increment in the wetted perimeter of the furrow caused an increase in the cumulative infiltration. These results are consistent with the results of Vogel and Hopmans (1992) and Abbasi et al. (2003). However, only an increase in cumulative infiltration is not adequate to obtain a high level of water application efficiency and water distribution uniformity in furrow irrigation. In the present investigation, increasing the wetted perimeter (P) in Eq. 19 increases the amount of infiltration (d). In addition, in the method proposed, maximization of the cross-sectional area of the wetting pattern where the net irrigation water requirement of the crop was met completely in the root zone and minimization of deep percolation are taken into consideration simultaneously. Therefore, a provision was made to determine the optimum length of the furrow and the cut-off time which provided a high level of water application efficiency (94.29% and 94.18%) and a high rate of water distribution uniformity (90% and 91.3%). These results indicate that the model proposed can be used in the design of a blocked end furrow system.

Saberi et al. (2020) determined the percentage of increase or decrease of the average design parameters of a furrow system in which the water requirement (storage) efficiency increased from 14.2 to 76.7%, and water application efficiency increased from 13.8 to 44.9% when the inflow rate was increased from 0 to 5.4%, the furrow length was increased from 23.2 to 66.9%, and the cut-off time was increased from 18.8 to 112%, respectively. Similarly, Ghahraman-Nezhad et al. (2016) determined that increasing the inflow rate and the cut-off time increased the water application efficiency in open ended furrows. Apart from this, it was indicated that increasing the inflow rate and decreasing the cut-off time caused a reduction in deep percolation. Navabian and Moslemi-Koochesfahani (2012) determined that increasing the inflow rate and the cut-off time increased the water requirement (storage) efficiency. In contrast, Yazdi et al. (2008) reported that reducing the inflow rate and increasing the furrow length improved water application efficiency and deep percolation. The reason for these results may be the different irrigation conditions. When the furrow length and inflow rate were reduced under constant cut-off time, the amount of water losses was reduced, and thereby the water application efficiency increased. These investigations achieve optimum design of the furrow system by the trial and error method. An investigation is made of the interaction with each other of the parameters which affect the design of a furrow system. Thus, the length of furrow, the inflow rate and the cut-off time are determined, providing the minimum deep percolation and the maximum water application efficiency. These components show different interactions under various irrigation conditions. In the present investigation, the parameters which affect the design of the furrow system are taken into consideration simultaneously. Therefore, the design process of the furrow system is carried out providing the optimum interaction between all the parameters. In conclusion, the optimum furrow length and the cut-off time which minimize deep percolation and provide maximum water application efficiency (94.29% and 94.18%) and water distribution uniformity (90% and 91.3%) are determined. This process is carried out by the analytical solution method, not by the trial and error technique. These results indicate that the method proposed in this investigation can be used in the design of a blocked end furrow system.

Mazarei et al. (2020) carried out an investigation to optimize the performance of the blocked end furrow irrigation method for inflow rates of 1.0, 1.5 and 2 L s^{-1} using the WinSRFR model. The objective function of the model is the optimization of performance by taking into consideration the application efficiency, water distribution uniformity and deep percolation. The highest performance was obtained by providing a 35.99% increment in the value of the objective function for a 250-m furrow length and 1.0 L s^{-1} inflow. When the length of the furrow was reduced from 250 to 200 m, a 39.8% increment occurred in the value of the objective function. In contrast, when the furrow length was changed to 300 m, the value of the objective function decreased by 7.7%. In addition, when the slope was changed from 0.04 to 0.03%, the value of the objective function decreased by 0.9%. When the slope was increased to 0.05%, the value of the objective function increased by 1.0%. The results of this investigation are generally similar to the results of Morris et al. (2015), Anwar et al. (2016), Akbar et al. (2016) and Nie et al. (2019). These results indicated that a reasonable combination of inflow rate and cut-off time increased the water application efficiency to 75–90%. In addition, Xu et al. (2019) reported that the value of water application efficiency was reduced by increasing the furrow length. Similar results were reported by Bai et al. (2010) and Chen et al. (2012). In the present investigation, such parameters and variables as horizontal movement properties of water, infiltration of water to the soil profile, inflow rate, net irrigation water requirement, cut-off time, furrow length, water application efficiency, moisture distribution uniformity in the soil profile, maximization of the cross-sectional area of the wetting pattern where the net irrigation water requirement of the crop is met completely in the root zone, the net infiltration period, and the amount of deep percolation, all of which affect the optimum design of the furrow system, are simultaneously and interactively taken into consideration in the proposed model solution procedure. Thus, the optimum cut-off time

and the furrow length which provide the maximum water application efficiency (94.29% and 94.18%) and the water distribution uniformity (90% and 91.3%), and which minimize the deep percolation, are determined by the proposed model using the analytical solution method. These results indicate that the model proposed can be used in the design of a blocked end furrow system.

Conclusions

The results of the model devised in this investigation for level furrows with blocked end were compared with the results of the existing (USDA SCS) method. According to the new method, the length of the furrow was found to be 171.02 m. This value is 2.27% different from the furrow length of 175.00 m which was obtained from the existing method. The water application efficiency was 93.7% for the furrow length of 175.00 m in the existing (conventional) method and increased to 94.29% for the furrow length of 171.02 m in the solution of the new method. In addition, the water distribution uniformity (CU) was obtained as 90% for the proposed model, which is classified in the "good" category. Also, a high level of water application efficiency and the water distribution uniformity were obtained from the solution of another application given in the Supplementary Materials.

Some important advantages of the proposed model can be stated as follows: the cross section of the wetting pattern, which occurs in the furrow at any moment of irrigation application, can be estimated by the proposed model because the components of the wetting pattern are described as functions of time. The second advantage is that the new model has enabled the optimum combination of the parameters which are effective in the design of the furrow system. Therefore, a high level of water application efficiency and water distribution uniformity along the furrow can be obtained. Apart from this, in the proposed model, the cross-sectional area of the wetting pattern where the net irrigation water requirement of the crop was met along the furrow has been maximized. Therefore, high levels of water application efficiency have been obtained. Another advantage of the new model is that, as the difference between the amounts of water which infiltrated the soil at the head and end of the furrow during the water application period is low, a high level of water distribution uniformity was obtained along the furrow. This also provided a reduction in the amount of deep percolation.

Most importantly, the proposed model performed the calculation procedure by an analytical solution technique without any need for the trial and error approach or a numerical solution. Therefore, the design process of the furrow system was made easier by the use of simpler and fewer equations.

In conclusion, the mathematical description of the movement properties of water in soil made it possible to design the blocked end furrow system without slope. The results from the proposed model indicated that the equations devised in this investigation represented the movement of water in the soil, and the results showed a compatible trend with this process.

Meanings of the symbols used in this investigation

Note: In the new method, different variables must have uniform units in their own categories in the same equation. For instance, if the unit of the size of an area is cm^2, the unit of the length variable must also be in cm in the same equation. If the unit of time is hours, the rate of change of the size of the area in the same formula must be in $cm^2\ h^{-1}$, infiltration velocity must be in $cm\ h^{-1}$ and changing acceleration of size of the area must be in $cm^2\ h^{-2}$. By considering this feature, the calculation process can be carried out for the desired unit sets in the new method.

a, b, c: Coefficients for the soil type according to the USDA-SCS infiltration groups.

A_1: The size of the wetted area caused by deep percolation at moment t of the irrigation application (cm^2).

A_2: The size of the dry area which has not yet been irrigated in the soil profile at moment t of the irrigation application (cm^2).

A_{DS}: Size of the wetted area caused by deep percolation in soil profile (cm^2).

A_T: Cross sectional area of the infiltration profile along the furrow during the period T_b from the beginning of the irrigation (cm^2).

b_b: Depth of water infiltrating the soil at the head of the furrow during the period T_b from the beginning of the irrigation (mm). (This unit can be converted to cm in the calculation process of the new model.)

b_{min}: The minimum width of a furrow set (m).

b_s: Depth of water infiltrating the soil at the end of the furrow during the infiltration period T_s (mm). (This unit can be converted to cm in the calculation process of the new model.)

D or d: The amount of water infiltrating the soil at any moment T of the irrigation (mm).

d_n or D_n: Net irrigation water requirement of the crop in any irrigation period (mm). (This unit can be converted to cm in the calculation process of the new model.)

d_s: Amount of deep percolation (mm).

d_t: Total amount of irrigation water to be applied (mm).

f, g: Coefficients for the advance features of water in the furrow according to the USDA-SCS infiltration groups.

I: Infiltration velocity (mm min^{-1}). (This unit can be converted to cm h^{-1}in the calculation process of the new model.)

i_b: Infiltration velocity of water in the soil at the head of the furrow (mm min^{-1}). (This unit can be converted to cm/h in the calculation process of the new model.)

i_s: Infiltration velocity of water in the soil at the end of the furrow (mm min^{-1}). (This unit can be converted to cm h^{-1} in the calculation process of the new model.)

K: The (coordinates of the) intersection point of the slopeless line showing the net irrigation water requirement of the crop (D_n), and the [b_b b_s] sloping line formed by water at the border of the wetted area pattern in the soil profile (Fig. 3).

L: Length of furrow (m). (This unit can be converted to cm in the calculation process of the new model.)

n: Manning roughness coefficient (n = 0.04 for furrow irrigation).

N_{max}: The maximum number of furrow sets which can be placed across the width of the plot.

n_{min}: The minimum number of furrows in one furrow set.

P: Wetted perimeter of the furrow (m).

Q: Discharge of water source (system discharge) (L s^{-1}).

q: The inflow to the furrow (L s^{-1}).

q_{max}: The maximum inflow to the furrow (L s^{-1}).

S_0: The average hydraulic slope (m m^{-1}).

T or t: Any time point from the beginning of the irrigation application (min).

T_0: Average infiltration period (min).

T_a: Irrigation period (min).

T_b: Elapsed time from the beginning of the irrigation (min).

T_i: Water advance period. Length of time necessary for water to reach the end of the furrow (min).

T_n: Net infiltration period. Length of time for infiltration of the net irrigation water requirement of the crop (min).

T_s: Infiltration period at the end of the furrow (min). The value of this parameter is determined by the formula ($T_s = T_b - T_i$).

v: Average advance velocity of water on soil surface in a horizontal direction (cm h^{-1}).

V_{ADS}: Rate of change of the size of the wetted area caused by deep percolation in the soil profile (cm^2 h^{-1}).

V_{AT}: Rate of change of the size of the wetted area in the soil profile at any moment t of the irrigation (cm^2 h^{-1}).

w: Distance between two furrows (m).

Supplementary Information The online version contains supplementary material available at https://doi.org/10.1007/s00271-022-00782-2.

References

Abbasi F, Adamsen FJ, Hunsaker DJ, Feyen J, Shouse P, Van Genuchten MT (2003) Effects of flow depth on water flow and solute transport in furrow irrigation: field data analysis. J Irrig Drain Eng 129:237–246

Adamala S, Raghuwanshi NS, Mishra A (2014) Development of surface irrigation systems design and evaluation software (SIDES). Comput Electron Agric 100:100–109. https://doi.org/10.1016/j.compag.2013.11.004

Akbar G, Ahmad MM, Ghafoor A, Khan M, Islam Z (2016) Irrigation efficiencies potential under surface irrigation farms in Pakistan. J Eng Appl Sci 35(2):15–23

Anwar AA, Ahmad W, Bhatti MT, Haq ZU (2016) The potential of precision surface irrigation in the Indus basin irrigation system. J Irrig Sci 34(5):379–396

Bai MJ, Xu D, Li YN, Pereira LS (2010) Stochastic modelling of basins micro topography: analysis of spatial variability and model testing. J Irrig Sci 28(2):157–172

Bautista E, Clemmens AJ, Strelkoff TS, Schlegel J (2009) Modern analysis of surface irrigation systems with WinSRFR. Agric Water Manag 96:1146–1154

Bautista E, Schlegel JL, Strelkoff TS (2012) WinSRFR 4.1 user manual. Arid Land Agricultural Research Cent. https://www.ars.usda.gov/ARSUserFiles/20200515/WinSRFR4_UserManual.pdf. Accessed Oct 2019

Bristow KL, Šimůnek J, Helalia SA, Siyal AA (2020) Numerical simulations of the effects furrow surface conditions and fertilizer locations have on plant nitrogen and water use in furrow irrigated systems. Agric Water Manag 232:106044

Burguete J, Lacasta A, García-Navarro P (2014) SURCOS: a software tool to simulate irrigation and fertigation in isolated furrows and furrow networks. J Comput Electron Agric 103:91–103

Chen B, Ouyang Z, Zhang SH (2012) Evaluation of hydraulic process and performance of border irrigation with different regular bottom configurations. J Resour Ecol 3(2):151–160

Delgoda D, Saleem SK, Malano H, Halgamuge MN (2016) Root zone soil moisture prediction models based on system identification: formulation of the theory and validation using field and AQUACROP data. Agric Water Manag 163:344–353

Dialameh B, Parsinejad M, Ebrahimian H, Mokhtari A (2018) Field comparison of infiltration in conventional and alternate Furrow irrigation under various initial and boundary conditions. Irrig Drain 67:156–165. https://doi.org/10.1002/ird.2176

Ebrahimian H (2014) Soil infiltration characteristics in alternate and conventional furrow irrigation using different estimation methods. KSCE J Civ Eng 18(6):1904–1911. https://doi.org/10.1007/s12205-014-1343-z (**pISSN 1226-7988, eISSN 1976-3808**)

Ebrahimian H, Ghaffari P, Ghameshlou AN, Tabatabaei SH, Dizaj AA (2020) Extensive comparison of various infiltration estimation methods for furrow irrigation under different field conditions. Agric Water Manag 230:105960

Esfandiari M, Maheshwari BL (2001) Field evaluation of furrow irrigation models. J Agric Eng Res 79(4):459–479. https://doi.org/10.1006/jaer.2001.0717

Ghahraman-Nezhad M, Borumand-Nasab S, Sheyni-Dashtgol A (2016) Determination of optimal design parameters for irrigation design by the WinSRFR3.1 model case study: South Ahwaz sugar cane fields. J Water Soil Sci 26(1.1):117–130

Gillies MH, Smith RJ (2015) SISCO: surface irrigation calibration and optimization. J Irrig Sci 33(5):339–355
Jurriens M, Zerihun D, Boonstra J (2001) SURDEV: surface irrigation software. J International Institute for Land Reclamation and Improvement, Wageningen
Kanber R, Ünlü M (2008) Türkiye'de Sulama ve Drenaj Sorunları: Genel Bakış. 5. Dünya Su Forumu Bölgesel Hazırlık Süreci DSİ Yurtiçi Bölgesel Su Toplantıları. T.C. Çevre ve Orman Bakanlığı, Devlet Su İşleri Genel Müdürlüğü, DSİ VI. Bölge Müdürlüğü. Sulama – Drenaj Konferansı Bildiri Kitabı (10–11 Nisan, Adana). s.1–45
Kang SZ, Shi P, Pan YH, Liang ZS, Hu XT, Zhang J (2000) Soil water distribution, uniformity and water-use efficiency under alternate furrow irrigation in arid areas. Irrig Sci 19:181–190
Katopodes ND (1994) Hydrodynamics of surface irrigation: vertical structure of the surge front. Irrig Sci 15:101–111
Kermani SG, Sayari S, Kisi O, Zounemat-Kermani M (2019) Comparing data driven models versus numerical models in simulation of waterfront advance in furrow irrigation. Irrig Sci 37:547–560. https://doi.org/10.1007/s00271-019-00635-5
Khatri KL, Smith RJ (2006) Real-time prediction of soil infiltration characteristics for the management of furrow irrigation. Irrig Sci 25:33–43. https://doi.org/10.1007/s00271-006-0032-1
Kilic M (2020) A new analytical method for estimating the 3D volumetric wetting pattern under drip irrigation system. Agric Water Manag 228(2020):105898. https://doi.org/10.1016/j.agwat.2019.105898
Kilic M, Anac S (2010) Multi-objective planning model for large scale irrigation systems: method and application. Water Resour Manag 24(12):3173–3194. https://doi.org/10.1007/s11269-010-9601-4
Kilic M, Anac S (2012) Sustainable management of large scale irrigation systems: a decision support model for Gediz Basin, Turkey. Sustainable Natural Resources Management (Chapter 3). InTech, New York. https://doi.org/10.5772/33120 (**ISBN: 978-953-307-670-6**)
Kilic M, Tuylu GI (2010) Determination of water conveyance loss in the Ahmetli Regulator irrigation system in the Lower Gediz Basin, Turkey. Irrig Drain. https://doi.org/10.1002/ird.602
Koech RK, Smith RJ, Gillies MH (2014) A real-time optimisation system for automation of furrow irrigation. Irrig Sci 32:319–327. https://doi.org/10.1007/s00271-014-0432-6
Levidow L, Zaccaria D, Maia R, Vivas E, Todorovic M, Scardigno A (2014) Improving water-efficient irrigation: Prospects and difficulties of innovative practices. Agric Water Manag 146:84–94
Liu K, Huang G, Xu X, Xiong Y, Huang Q, Šimůnek J (2019) A coupled model for simulating water flow and solute transport in furrow irrigation. Agric Water Manag 213(2019):792–802
Mailhol JC, Ruelle P, Popova Z (2005) Simulation of furrow irrigation practices (SOFIP): a field-scale modelling of water management and crop yield for furrow irrigation. Irrig Sci 24:37–48. https://doi.org/10.1007/s00271-005-0006-8
Mazarei R, Mohammadi AS, Naseri AA, Ebrahimian H, Izadpanah Z (2020) Optimization of furrow irrigation performance of sugarcane fields based on inflow and geometric parameters using WinSRFR in Southwest of Iran. Agric Water Manag 228:105899. https://doi.org/10.1016/j.agwat.2019.105899
Mazarei R, Mohammadi AS, Ebrahimian H, Naseri AA (2021) Temporal variability of infiltration and roughness coefficients and furrow irrigation performance under different inflow rates. Agric Water Manag 245:106465. https://doi.org/10.1016/j.agwat.2020.106465
Montesinos P, Camacho E, Alvarez S (2001) Seasonal furrow irrigation model with genetic algorithms (OPTIMEC). Agric Water Manag 52:1–16
Morris MR, Hussain A, Gillies MH, Halloran NJ (2015) Inflow rate and border irrigation performance. J Agric Water Manag 155:76–86
Naghedifar SM, Ziaei AN, Ansari H (2020) Numerical analysis and optimization of triggered furrow irrigation system. Irrig Sci 38:287–306. https://doi.org/10.1007/s00271-020-00672-5
Navabian M, Moslemi-Koochesfahani M (2012) Optimization of furrow length and inflow rate in furrow irrigation. Iran J Water Res 6(11):27–34
Nie WB, Fei LJ, Ma XY (2014) Impact of infiltration parameters and Manning roughness on the advance trajectory and irrigation performance for closed-end furrows. Span J Agric Res 12:1180–1191
Nie WB, Li YB, Zhang F, Dong SX, Wang H, Ma XY (2018) A method for determining the discharge of closed-end furrow irrigation based on the representative value of Manning's roughness and field mean infiltration parameters estimated using the PTF at regional scale. Water 10:1825. https://doi.org/10.3390/w10121825
Nie WB, Li YB, Zhang F, Ma XY (2019) Optimal discharge for closed-end border irrigation under soil infiltration variability. J Agric Water Manag 221:58–65
Piazentin JC, Zocoler JL, Cremasco CP, Neto AB, Filho LRAG (2019) Water distribution uniformity in driping system under growing pressures. Int J Innov Educ Res 7(11):14–21. https://doi.org/10.31686/ijier.Vol7.Iss11.1829
Pozo AD, Brunel-Saldias N, Engler A, Ortega-Farias S, Acevedo-Opazo C, Lobos GA, Jara-Rojas R, Molina-Montenegro MA (2019) Climate change impacts and adaptation strategies of agriculture in Mediterranean-climate regions (MCRs). Sustainability 11:2769. https://doi.org/10.3390/su11102769
Raghuwanshi NS, Wallender WW (1999) Forecasting and optimizing furrow irrigation management decision variables. Irrig Sci 19:1–6
Saberi E, Siuki AK, Pourreza-Bilondi M, Shahidi A (2020) Development of a simulation–optimization model with a multi-objective framework for automatic design of a furrow irrigation system. Irrig Drain 69:603–617. https://doi.org/10.1002/ird.2460
Salahou MK, Jiao XY, Lü HS (2018) Border irrigation performance with distance-based cut-off. Agric Water Manag 201:27–37
Sayari S, Rahimpour M, Zounemat-Kermani M (2017) Numerical modelling based on a finite element method for simulation of flow in furrow irrigation. J Paddy Water Environ 15(4):879–887
USDA SCS (2012) Surface irrigation, chapter 4, part 623, irrigation. National engineering handbook. https://directives.sc.egov.usda.gov/OpenNonWebContent.aspx?content=39787.wba. Accessed May 2018
Selle B, Minasny B, Bethune M, Thayalakumaran T, Chandra S (2011) Applicability of Richards' equation models to predict deep percolation under surface irrigation. Geoderma 160:569–578
Šimůnek J, van Genuchten MT, Šejna M (2008) Development and applications of the HYDRUS and STANMOD software packages and related codes. Vadose Zone J 7(2):587–600. https://doi.org/10.2136/VZJ2007.0077
Šimůnek J, van Genuchten MT, Šejna M (2016) Recent developments and applications of the HYDRUS computer software packages. Vadose Zone J 15(7):25. https://doi.org/10.2136/vzj2016.04.0033
Smith RJ, Uddin MJ, Gillies MH (2018) Estimating irrigation duration for high performance furrow irrigation on cracking clay soils. Agric Water Manag 206:78–85
Valiantzas JD (2000) Surface water storage independent equation for predicting furrow irrigation advance. Irrig Sci 19:115–123
Vogel T, Hopmans JW (1992) Two-dimensional analysis of furrow infiltration. J Irrig Drain Eng 118:791–806
Walker WR (2003) SIRMOD III-surface irrigation simulation, evaluation and design: guide and technical documentation. Department of Biological and Irrigation Engineering, Utah St. University Logan, Logan
Walker WR, Skogerboe GV (1987) Surface irrigation theory and practice. Prentice-Hall Inc, Englewood Cliffs, p 386
Wang J, Huang G, Zhan H, Mohanty BP, Zheng J, Huang Q, Xu X (2014) Evaluation of soil water dynamics and crop yield under furrow

irrigation with a two-dimensional flow and crop growth coupled model. Agric Water Manag 141:10–22

Wu D, Xue J, Bo X, Meng W, Wu Y, Du T (2017) Simulation of irrigation uniformity and optimization of irrigation technical parameters based on the SIRMOD model under alternate furrow irrigation. J Irrig Drain Eng 66(4):478–491

Xu J, Cai H, Saddique Q, Wang X, Li L, Ma C, Lu Y (2019) Evaluation and optimization of border irrigation in different irrigation seasons based on temporal variation of infiltration and roughness. J Agric Water Manag 214:64–77

Yazdi Z, Mohseni-Movahed SA, Heydari M (2008) Preparation of a model for evaluation, design, simulation and optimization of the furrow irrigation. In: Article collection of the second seminar on improvement and correction of surface irrigation systems. Hall of Collections of Karaj Research Institutions, pp 121–136

Yıldırım O (2013) Design of irrigation systems (4th press). Ankara University Faculty of Agriculture, Department of Agricultural Structures and Irrigation, Ankara (**no:1594, book: 546**)

Zerihun D, Feyen J, Reddy JM (1997a) Empirical functions for dependent furrow irrigation variables. 1. Methodology and equations. Irrig Sci 17:111–120

Zerihun D, Wang Z, Feyen J, Reddy JM (1997b) Empirical functions for dependent furrow irrigation variables. 2. Applications. Irrig Sci 17:121–126